Published in final edited form as:
Dev Biol. 2012 September 1; 369(1): 43–53. doi:10.1016/j.ydbio.2012.06.017.

cSrc is necessary for epididymal development and is incorporated into sperm during epididymal transit

Dario Krapf[a,b], **Ye Chun Ruan**[c], **Eva V. Wertheimer**[a], **Maria A. Battistone**[d], **John B. Pawlak**[a], **Archana Sanjay**[e], **Stephen H. Pilder**[f], **Patricia Cuasnicu**[d], **Sylvie Breton**[c], and **Pablo E. Visconti**[a,1]

[a]Department of Veterinary and Animal Science, University of Massachusetts, Amherst, MA 01003, USA

[b]Institute of Molecular and Cell Biology of Rosario (CONICET-UNR), S2002LRK Rosario, Argentina

[c]Program in Membrane Biology and Center for Systems Biology, Massachusetts General Hospital and Harvard Medical School

[d]Instituto de Biologia y Medicina Experimental, CONICET, C1428ADN Buenos Aires, Argentina

[e]University of Connecticut Health Center, New England Musculoskeletal Institute, Department of Orthopaedic Surgery, Farmington, CT 06030

[f]Dept. of Anatomy and Cell Biology, Temple University School of Medicine, Philadelphia, PA 19140

Abstract

Changes that occur to mammalian sperm upon epididymal transit and maturation render these cells capable of moving progressively and capacitating. Signaling events leading to mammalian sperm capacitation depend on the modulation of proteins by phosphorylation and dephosphorylation cascades. Recent experiments have demonstrated that the Src family of kinases plays an important role in the regulation of these events. However, sperm from cSrc null mice display normal tyrosine phosphorylation associated with capacitation. We report here that, despite normal phosphorylation, sperm from cSrc null mice display a severe reduction in forward motility, and are unable to fertilize in vitro. Histological analysis of seminiferous tubules in the testes, caput and corpus epididymis do not reveal obvious defects. However, the cauda epididymis is significantly smaller, and expression of key transport proteins in the epithelial cells lining this region is reduced in cSrc null mice compared to wild type littermates. Although previously, we and others have shown the presence of cSrc in mature sperm from cauda epididymis, a closer evaluation indicates that this tyrosine kinase is not present in sperm from the caput epididymis, suggesting that this protein is acquired by sperm later during epididymal maturation. Consistent with this observation, cSrc is enriched in vesicles released by the epididymal epithelium known as epididymosomes. Altogether, these observations indicate that cSrc is essential for cauda epididymal development and suggest an essential role of this kinase in epididymal sperm maturation involving cSrc extracellular trafficking.

[1]Address correspondence to: Pablo E. Visconti, 661 North Pleasant ST, Amherst, MA 01003; Tel.: 413-545-5565; Fax: 413-545-6326; pvisconti@vasci.umass.edu.

Keywords

epididymal maturation; extracellular trafficking; Src kinase; sperm capacitation; sperm motility

INTRODUCTION

After leaving the testis, mammalian sperm are immotile and are unable to fertilize, requiring that they undergo two post-testicular processes known as sperm maturation and capacitation, in order to gain fertilizing ability. Sperm maturation occurs during epididymal transit. The epididymis is a pseudostratified epithelium that can be anatomically differentiated into four main regions: initial segments, caput, corpus and cauda starting with the proximal initial segment being the region closest to the efferent ducts which connect the testis to the epididymis. The main epididymal function is to provide an environment suitable for sperm maturation, transport, and storage. During epididymal maturation, a series of physiological changes allow sperm to become progressively motile and capacitation-competent (see below). The molecular basis of epididymal sperm maturation is not well understood; however, changes in the sperm membrane composition (Abascal et al. 1998), mainly as a result of incorporation of epididymal proteins (Caballero et al. 2010) appear to be an essential element of this process. After epididymal maturation, sperm are required to undergo a capacitation process in the female reproductive tract in order to become competent to fertilize the egg. Sperm capacitation is associated with functional parameters such as alteration of motility patterns and acrosomal responsiveness (Visconti et al. 2011). At the molecular level, these functional changes correlate with the activation of a phosphorylation cascade involving an increase in tyrosine phosphorylation mediated by the activation of a cAMP/PKA pathway (Visconti et al. 1995). Despite advances in our understanding of the role of phosphorylation in sperm capacitation, the identity of the tyrosine kinase(s) responsible for the capacitation-associated increase in tyrosine phosphorylation had remained obscure until recent studies suggested that cSrc was the tyrosine kinase involved in this process (Baker et al. 2006). Supporting this conclusion, results from our group showed that cSrc is activated during sperm capacitation and known inhibitors of cSrc family kinases (SFK) such as SU6656 and SKI606 block sperm capacitation and the associated increase in phosphorylation (Krapf et al. 2010). However, we also demonstrated that SFK inhibition can be overcome by addition of okadaic acid, indicating that SFK are not directly involved in the general onset of tyrosine phosphorylation (Krapf et al. 2010). Moreover, an increase in tyrosine phosphorylation was evident in capacitated sperm from cSrc null mice.

Interestingly, investigators have shown previously that cSrc null mice are sterile in vivo (Schwartzberg et al. 1997). However, it is highly likely that the osteopetrotic status of cSrc null mice negatively affects their reproductive behavior, leading to their impaired fertility (Soriano et al. 1991). In addition, progressive odontoma growth causes gradual airway obliteration, leading to a loss of activity and eventual death by suffocation of these animals (Amling et al. 2000). Thus, the high rates of morbidity and mortality hamper detailed analysis of Src functions in various organ systems, especially the male reproductive tract. While we and others have shown that with a normal diet cSrc null mice die usually within five weeks of birth because of an inability to feed on solid food, animals maintained on a soft food/liquid diet usually survive for at least 4–5 months, allowing some of them to reach sexual maturity. In this regard, we have previously shown that the capacitation-associated increase in tyrosine phosphorylation is not affected in sperm from cSrc null mice (Krapf et al. 2010). However, in the present study, we show that sperm from cSrc knockout (KO) mice have significantly reduced motility and are unable to fertilize in vitro. Their testes, caput and corpus epididymides appear normal; however, the cauda epididymis in cSrc KO

mice is significantly smaller when compared to its counterpart in either KO heterozygotes or wild type mice. A more detailed analysis has revealed that cSrc is highly expressed in epididymal clear cells and more weakly expressed in principal cells. In cSrc null cauda epididymis, principal cells and clear cells have reduced expression of AQP9 and V-ATPase, respectively (two specific markers for these cell types) and clear cells are smaller compared to those of wild type epididymides. In addition to these observations, we report that during spermatogenesis cSrc was absent from late developing spermatids, and was not found in caput sperm. However, in cauda sperm, cSrc was observed by western blot and immunofluorescence. Taking into consideration that sperm are transcriptionally and translationally inactive, this observation suggests that this signaling protein is acquired during epididymal maturation. Altogether, these new data demonstrate an essential role for cSrc in epididymal development, and strongly suggest that it is also responsible for major maturational changes of spermatozoa that occur during epididymal transit.

MATERIALS AND METHODS

Materials

Chemicals were obtained from the following sources: Bovine serum albumin (BSA, fatty acid-free) was purchased from Sigma (St. Louis, MO). SU6656 was obtained from Calbiochem, okadaic acid was acquired from LC Labs (Woburn, MA). Anti-phosphotyrosine (pY) monoclonal antibody (clone 4G10) was obtained from Upstate Biotechnology (Lake Placid, NY). Rabbit monoclonal anti-phosphoPKA substrates (clone 100G7E) and anti-Src monoclonal antibodies (clone 32G6) were purchased from Cell Signaling (Danvers, MA). Anti-β-tubulin monoclonal antibody (clone E7) was obtained from the Developmental Studies Hybridoma Bank developed under the auspices of the National Institutes of Health, NICHD, and maintained by The University of Iowa Department of Biological Sciences, Iowa City, IA. Anti-GFP mouse mAb (Cat# MAB3580) was purchased from Millipore (Bedford, MA). Horseradish peroxidase-conjugated anti-mouse and anti-rabbit IgG were purchased from Jackson Immunoresearch Laboratories (West Grove, PA) and Amersham (GE Healthcare) respectively.

Mouse Sperm Preparation

Animals were sacrificed in accordance with the Animal Care and Use Committee guidelines of UMass-Amherst or Temple University School of Medicine. Cauda epididymal mouse sperm were collected from CD1 retired male breeders (Charles River Laboratories, Wilmington, MA), from young adult (7–8 week-old) cSrc-null males and their wild-type littermates were maintained at Temple Med Animal Facility (commercially available at Jackson Labs B6;129S7-*Src*^{tm1Sor}/J)(Soriano et al. 1991), or from Acr-GFP CF1 transgenic male mice (7- to 8-weeks old) (Nakanishi et al. 1999). Each minced cauda epididymis was placed in 500 μl of a modified Krebs-Ringer medium (Whitten's HEPES-buffered medium containing 5 mg/ml BSA) (Moore et al. 1994). After 10 min incubation at 37°C, epididymides were removed, and the suspension adjusted with non-capacitating medium to a final concentration of 1–2 × 10^7 cells/ml before 4× dilution in the experimentally appropriate medium. For capacitation, 15 mM $NaHCO_3$ was added, and sperm incubated at 37°C for at least 1 h. To test the effect of inhibitors on capacitation, sperm were pre-incubated with inhibitors in non-capacitating medium for 15 min prior to the beginning of the capacitating period. For in vitro fertilization (IVF) assays, sperm were first capacitated in Whitten's medium without HEPES containing 22 mM $NaHCO_3$ and 5 mg/ml BSA, previously equilibrated in a humidified atmosphere of 5% CO2 at 37°C (Wertheimer et al. 2008).

In experiments where cauda and caput sperm were compared for the presence of cSrc, both caput and cauda sperm were purified using Percoll gradients. The caput region of the epididymis was dissected and placed in a 200 μl drop of Whitten's medium. Multiple incisions were then made in the tissue with a 26G needle and sperm gently squeezed out into the medium. Cauda sperm were obtained as described above. For each population, the resultant cell suspension was diluted to 1 ml containing 2–5 × 10^6 cells. This suspension was layered over 4 ml of Percoll, consisting of a 90% Percoll lower phase and a 45% Percoll upper phase in PBS, and centrifuged at 650×*g* for 25 min at RT. The interphase between the two Percoll phases contained washed caput sperm, which were collected and further diluted 1–2 × 10^7 cells/ml. The Percoll-purified population was used for Western blot and immunofluorescence analyses.

SDS-PAGE and immunoblotting

Sperm were collected by centrifugation, washed in 1 ml of PBS, resuspended in Laemmli sample buffer (Laemmli, 1970), and boiled for 5 min. After centrifugation, 5% β-mercaptoethanol was added to the supernatants and boiled again for 5 min. Protein extracts equivalent to 1–2 × 10^6 sperm per lane were analyzed by western blot as described (Krapf et al. 2010). Antibodies were diluted in TBS containing 0.1% Tween-20 as follows: 1/105,000 for anti-PY (clone 4G10), 1/5,000 for anti-pPKA (clone 100G7E), 1/1,000 for anti-Src antibodies (clone 32G6), and 1/10,000 for anti-tubulin (clone E7), anti-PY, anti-GFP, and anti-actin. Secondary antibodies were diluted 1/10,000 in T-TBS and developed using an enhanced chemiluminescence detection kit (ECL plus, Amersham, GE Healthcare) according to the manufacturer's instructions. When necessary, PVDF membranes were stripped as described (Krapf et al. 2010).

Sperm Motility Analysis

Sperm suspensions were loaded on a 20-μm chamber slide (Leja slide, Spectrum Technologies) and placed on a microscope stage at 37 °C. Sperm movements were examined using the CEROS computer-assisted semen analysis (CASA) system (Hamilton Thorne Research, Beverly, MA) as described (Wertheimer et al. 2008).

Mouse Eggs Collection and IVF Assays

Metaphase II-arrested eggs were collected from 6-8 week-old superovulated C57BL/6 female mice (Charles River Laboratories) at 13 h after human chorionic gonadotrophin (Sigma) ip injection. IVF were performed on cumulus free eggs as described previously (Wertheimer et al. 2008). Briefly, fertilization drops (200 μl each) containing 10–20 eggs were inseminated with capacitated sperm (final concentration of 2.5 × 10^6 cells/ml). Fertilization was assessed by visualization of the formation of the male and female pronuclei.

Epididymal fluid and epididymosomes

To obtain cauda epididymal fluid, sperm were allowed to swim out of cauda epididymides into PBS for 10 min. Epididymides were removed, and the suspension centrifuged at 2300×*g* for 10 min at 4° C to remove sperm. Luminal fluid was further clarified by centrifugation at 10,000×*g* for 20 min at 4°C. The resultant supernatant was called epididymal fluid and stored at −20°C. Epididymosomes were isolated by further centrifuging epididymal fluid at 120,000×*g* for 2 hrs at 4°C using a Beckman Coulter Ti90 rotor. The epididymosome containing pellet was resuspended in PBS, to final concentration of 1–1.5 mg/ml of total proteins.

Transmission Electron Microscopy

Vesicles were placed on Formvar membrane and carbon coated copper or nickel TEM grids, fixed in 4% paraformaldehyde, washed in filtered PBS, rinsed in H_2O and stained with phosphotungstic acid. Images were taken using an EM 10C, Zeiss. For spermatozoa, previously described methods were used (Pilder et al. 1993).

Immunohistochemistry

Epididymides and testes from young adult (7–8 week-old) cSrc-null males and their wild-type littermates (Soriano et al. 1991) were fixed by immersion in periodate–lysine–paraformaldehyde (PLP) containing 2% paraformaldehyde for 5 h at room temperature and weighed. PLP-fixed tissues were cryoprotected in a solution of 30% sucrose in PBS. Tissues were embedded in OCT compound (Tissue-Tek; Sakura, Finetek USA, Torrance, CA, USA), mounted on a cutting block, and frozen in a Reichert Frigocut or a Leica 3050 cryotome (spencer Scientific). The tissue was then cut at 4 m thickness, and sections were placed onto Fisher Superfrost Plus microscope slides (Fisher Scientific, Pittsburgh, PA, USA). After rehydration in PBS at room temperature, all tissue slides were pretreated with 1% SDS for 4 min, as previously described (Brown et al. 1996). The slides were then washed in PBS (3×5 min) and pre-incubated in 1% BSA in PBS/0.02% sodium azide for 15 min at room temperature to block nonspecific staining. Anti-AQP9 rabbit antibody (Pastor-Soler et al. 2002), anti-Src antibody and anti-V-ATPase B1 subunit chicken antibody (Shum et al. 2011) were prepared at dilutions of 1:500, 1:100 and 1:100 respectively in antibody diluent (DAKO, Carpinteria, CA, USA) and applied for 75 min at room temperature. The slides were then washed twice for 5 min in high salt PBS (2.7% NaCl) to reduce nonspecific staining, and once in normal PBS. Secondary antibodies were goat anti-rabbit IgG coupled to FITC (1:60) or Cy3 (1:800) and donkey anti-chicken coupled to FITC (1:60) or Cy3 (1:800), and were applied for 1 h at room temperature (Jackson Immunologicals, West Grove, PA, USA), followed by three washes as described for the primary antibody. The slides were mounted in Vectashield (Vector Labs, Burlingame, CA, USA) diluted 1:1 in Tris buffer pH 8.5 and examined using a Nikon E800 epifluorescence microscope. Digital images were obtained using a Hamamatsu Orca CCD camera and IPLab Spectrum software (Scanalytics, Vianna, VA, USA). For experiments showing cSrc and V-ATPase B1 subunit in different developmental stages, wild type ICR male mice (Jackson Labs, Bar Harbor, ME) were used.

Quantification of AQP9 and B1 ATPase expression by immunofluorescence labeling

Immunofluorescence labeling of each tissue was performed in at least three independent incubations, each incubation including slides from all groups. All slides for a particular incubation were treated under identical conditions, and digital images were obtained using identical acquisition parameters. Each image was corrected for its own luminal unstained background value, and the mean pixel intensity (MPI) of apical AQP9 and B1 ATPase associated fluorescence were measured using IPLab Spectrum software. This method has been previously used to quantify the regulation of epididymal AQP9 expression by steroid hormones in rats (Pastor-Soler et al. 2010;Pastor-Soler et al. 2002).

Quantitative Real-Time RT-PCR

Epididymal tissues from 1–8 week male mice (wild type ICR, Jackson Labs, Bar Harbor, ME) were minced with a razor and with the aid of a 18G needle in PBS in RNase-free conditions and used to isolate total RNA using High Pure RNA Isolation Kit protocol (Roche, cat #11828665001), according to manufacturer's directions. cDNA synthesis was performed with SuperScript III First-Strand Synthesis System for RT-PCR (Invitrogen, cat #18080-051), using oligo(dT)20, following manufacturer's instructions. Real-time RT-PCR

was performed using 60 ng of cDNA with Taqman probe based gene expression assays from Applied Biosystems, using PerfeCTa Supermix Low ROX (Quanta Biosciences, cat #95052), Vic-labeled GAPDH Taqman Assay (Cat #Mm99999915_g1), FAM-labeled Src Taqman Assay (Cat #Mm00436785_m1) and nuclease free water in a final volume of 20 μL. Reactions were run in triplicate on a Stratagene Mx3005p Real-Time PCR machine with a thermal profile of: 1 cycle of 95°C for 2 minutes, then 40 cycles of 15 seconds at 95°C and 60 seconds at 60°C.

Statistical Analysis

Paired or unpaired Student's t test was used for compairing mean values between control and tested groups. The difference between mean values of multiple groups was analyzed by one-way analysis of variance followed by Holm-Sidak test. Statistical significances are indicated in figure legends.

RESULTS

Caudae epididymides in cSrc null mice are smaller than in wild type mice

During sperm preparation procedures, it was evident that the epididymides from cSrc-null mice were smaller than those from wild type siblings (Fig. 1 A and B). This difference was limited to the cauda epididymal region (Fig. 1A). However, no difference in size or weight was observed in the testes (Fig. 1A; inset and 1B). These observations opened the possibility of a role for cSrc in epididymal function. Consistent with this hypothesis, immunofluorescence localization experiments indicated the presence of cSrc in the epididymis. In mammals, the epithelial lining of the epididymis consists of several cell types. Among them, principal and clear cells are the most abundant. cSrc immunostaining revealed that the protein is present in both types of cells, but is more abundant in clear cells, identified by their positive labeling for the V-ATPase subunit B1 (Da Silva et al. 2010) (Fig. 2, left panels). As expected, cSrc null epididymides did not exhibit cSrc immunostaining (Fig. 2, right panels). Interestingly, clear cells exhibit a weaker V-ATPase B1 labeling and appear smaller in cSrc null compared to wild type epididymides. Observation at low magnification demonstrated that the distal cauda was smaller in cSrc null mice than in wild type mice (Figs 3A, B). At a higher magnification, double-labeling for aquaporin 9 (AQP9), a marker of principal cells (Pastor-Soler et al. 2010), and the V-ATPase B1 subunit confirmed the lower expression of B1 in clear cells of the proximal and distal cauda, and in the proximal ductus deferens of cSrc null mice (Figs 3D, F, H) compared to wild type mice (Figs 3C, E, G). The expression of AQP9 was significantly lower in the distal cauda (Fig. 3F) and proximal ductus deferens (Fig. 3H) of null mice compared to WT mice (Figs 3E, G). In the proximal cauda, no difference in AQP9 expression was observed between cSrc null and wild type mice (Fig. 3D versus 3C). Quantification analysis confirmed the reduced expression of AQP9 and B1 in several epididymal regions (Figs 3J, K) and the smaller size of clear cells in the proximal cauda epididymis of cSrc null compared to wild-type mice (Fig. 3L). Altogether these observations suggest that the absence of cSrc in null mice has repercussions for development of epithelial cells lining the distal regions of the epididymis and into the ductus deferens.

Expression of cSrc in epididymis of pre-adult mice

The finding that epididymides of cSrc null mice showed abnormal morphology led us to hypothezise that cSrc should be expressed before puberty in mouse epididymis to support its normal development. Epididymides from 1 to 8 weeks old mice were obtained and analyzed for *cSrc* expression by exon spanning quantitative PCR to visualize mRNA levels. As shown in Figure 4, expression of *cSrc* could be observed as early as 1 week after birth, doubling its expression levels at 2 to 6 weeks old, and lowering again at 8 weeks old. In order to gain

insight into the cell types expressing cSrc in epididymides from different post-natal stages, cSrc along with V-ATPase B1 subunit were tracked in histological sections (Fig 5). As clearly shown, cSrc is detected in all epithelial cells throughout the entire epididymis at both postnatal weeks 1 and 2, further demonstrating its high expression at these stages. A B1-labeled clear cell is already visible in the middle region at postnatal week 1 (arrow), whereas at postnatal week 2 B1-labeled clear cells are observed in all epididymal regions (arrows). In the following stages, at weeks 3 and 4, where each of the epididymal segments are clearly identifiable, cSrc was detected in clear cells (B1 positive) and principal cells in all segments, but preferentially localized to the apical membrane. At week 8, when mice reach puberty, the cSrc apical membrane labeling of principal cells decreased in some regions of the initial segment, corpus and distal cauda. At weeks 3, 4 and 8 cSrc is enriched in clear cells compared to principal cells of corpus, proximal and distal cauda. cSrc null sperm have significantly reduced motility and are unable to fertilize in vitro.

Since cSrc null mice showed altered epididymal morphology, and considering the role of the epididymis in sperm maturation, sperm fertility parameters were analyzed in cSrc KO mice. Interestingly, sperm released from the cauda epididymides of cSrc null mice showed poor motility (Fig. 6A and Table 1), consistent with one of the roles of the epididymis in supporting sperm maturation. Previously we have shown that SFK inhibitors negatively affected sperm motility in wild type sperm, and low concentrations of okadaic acid restored normal motility (Krapf et al. 2010). However, okadaic acid did not restore motility of cSrc null mouse sperm (Table 1). Moreover, the PKA-dependent increase in tyrosine phosphorylation in wild type sperm was also blocked in the presence of SFK inhibitors, but was restored in the presence of low concentrations of okadaic acid. These experiments indicated that in addition to the well-characterized bicarbonate activation of the soluble adenylyl cyclase (Adcyc10, aka SACY) in sperm, another pathway involving down-regulation of ser/thr phosphatases was necessary for sperm capacitation. To investigate whether this alternative pathway was also active in cSrc null sperm, both heterozygous and knock-out sperm were incubated under conditions that either support or do not support capacitation in the presence or in the absence of 50 μM of the SFK inhibitor, SU6656, for 60 min. Under these conditions, even in the absence of cSrc, SU6656 was able to reduce PKA-dependent phosphorylation and block the capacitation-associated increase in tyrosine phosphorylation (Fig. 6B). In both cases, addition of 1 nM okadaic acid overcame the inhibition, suggesting that SFK acts to down regulate ser/thr phosphatase(s). Despite these findings, KO sperm displayed negligible hyperactivated motility (Fig. 6C) and were unable to fertilize in vitro (Fig. 6D). No ultrastructural alterations that might explain the motility defects were observed in KO spermatozoa when compared to wild-type spermatozoa (Fig. S1).

cSrc is incorporated into sperm during epididymal transit

Previous studies by our group using western blot analyses (Krapf et al. 2010), as well as by others (Baker et al. 2006), showed that cSrc is present in mature sperm. Because of the abundance of cSrc in epididymal cells, the presence of this tyrosine kinase in sperm was re-evaluated in Percoll purified sperm to avoid contamination with epididymal tissue. Results from caudal sperm revealed that cSrc is present in mature sperm; however, this kinase was completely absent from sperm obtained from the caput epididymal region (Fig. 7A, left panel). Equal loading of sperm was validated using anti-tubulin western blots and the tyrosine phosphorylated form of hexokinase type I, which is independent of the sperm capacitation status (Platt et al. 2009;Kalab et al. 1994). In addition, as a second sperm-specific marker, the same experiment was conducted using spermatozoa from transgenic mice expressing GFP in their acrosomes (Nakanishi et al. 1999). This control was done in order to exclude the possibility of acrosomal loss during Percoll gradient washing. Using

caput and caudal sperm from these mice the same results were observed (Fig. 7B), and equal loading was verified using tubulin, tyrosine phosphorylated hexokinase and GFP. In addition, the status of the acrosome was evaluated and no differences were found after percoll purification in caput or cauda sperm (Fig. S2); other controls establishing that Percoll wash was necessary to avoid epididymal contamination are presented in Figure S3. Consistent with these results, immunofluorescence experiments revealed that cSrc is present in mature caudal sperm in the midpiece and postacrosomal regions, but specific staining for this kinase was completely absent from caput sperm (fig. 7C). As controls for the specificity of the antibody, cSrc null sperm were used. Similar to caput sperm, only a non-specific reaction in the sperm annulus was observed.

Since cSrc is absent from caput sperm, we hypothesized that this protein should also be absent in condensed spermatids. To analyze the fate of cSrc during spermiogenesis, spermatogenic cell fractions were obtained using a Staput (Bellve et al. 1977), and the presence or absence of cSrc was determined by western blot analysis. While cSrc was observed in pachytene spermatocytes, the presence of this kinase decreases in round spermatids, and is barely visible at best in condensed spermatids (Fig. 8A). Because they are transcriptionally and translationally inactive after leaving the testis, sperm are unable to synthesize new proteins. Therefore, the most likely explanation for the presence of cSrc in cauda epididymal sperm is that cSrc is incorporated into the cells during epididymal maturation. Although the mechanism of protein incorporation during epididymal sperm maturation is not completely understood, it is believed that it occurs via sperm membrane fusion with small exosomal vesicles (known as epididymosomes), released by the epididymis (Sullivan et al. 2007). To evaluate this possibility, sperm-free epididymal fluid and purified epididymosomes were evaluated for the presence of cSrc (Fig. 8B). The purity of the epididymosome fraction was determined by electron microscopy (Fig. 8C). This experiment indicated that cSrc is present in epididymal fluid, and is enriched in epididymosomes. It has been suggested that upon transfer to sperm, epididymal proteins behave as membrane proteins (Kirichok et al. 2006), or they are incorporated into the intracellular structures of spermatozoa (Frenette and Sullivan, 2001). In the case of cSrc, subcellular fractionation revealed that this tyrosine kinase is enriched in membrane fractions (Fig. 8D). This result is consistent with cSrc membrane localization in other cell types (Donepudi and Resh, 2008).

DISCUSSION

After completing morphological differentiation in the testis, mammalian sperm are unable to move or fertilize eggs. They need to undergo a maturation process in the epididymis and capacitation in the female reproductive tract before acquiring full fertilization competency. We have previously shown that sperm from cSrc null mice are capable of undergoing capacitation-associated changes in protein tyrosine phosphorylation (Krapf et al. 2010). Despite these findings, cSrc null males are sterile (Schwartzberg et al. 1997); however, in this previous work the reproductive phenotype was not analyzed and sterility could have been due to defects in mating behavior. In the present work we report that sperm from cSrc null mice have significantly reduced motility and are incapable of fertilizing in vitro. In addition, analysis of the cSrc null reproductive phenotype reveals defects in the epididymal epithelium. The epididymis is divided into four main sections: initial segments, caput, corpus and cauda, which contain several epithelial cell types. The four major epithelial cell types have been referred to as principal, narrow, basal, and clear cells based on structural and functional parameters. Principal cells localize throughout the entire epididymis, narrow and clear cells are intercalated between principal cells, and basal cells are located at the base of the epithelium in the entire epididymis. Narrow cells are relatively low in number and are located in the initial segments. Clear cells, which are more numerous than narrow cells, are

located in the caput, corpus, and cauda epididymidis. Altogether, these cells are essential to establish and maintain a favorable environment for sperm maturation. During their transit in the epididymis, spermatozoa are in contact with a luminal environment that continually changes along the length of the duct as a result of secretory and absorptive processes across the epithelium (Cornwall, 2009;Robaire et al. 2006). Clear cells are significant contributors to the establishment of a luminal acidic pH, which is achieved via the proton pumping V-ATPase. Together with a low bicarbonate concentration, this low pH helps keep spermatozoa in a quiescent state during their maturation and storage (Shum et al. 2011). Principal cells are involved in ion and fluid transport across the epididymal epithelium. AQP9 in these cells is the predominant water channel in the epididymis and participates in the control of the fluidity of the luminal content (Badran and Hermo, 2002;Pastor-Soler et al. 2001;Elkjaer et al. 2000). Moreover, AQP9 is permeant to neutral solutes in addition to water and previous studies have indicated that it mediates the transport of key sperm substrates, including glycerol, in the epididymis (Pietrement et al. 2008). In addition, it is thought that epididymal secretions function to protect, stabilize and modify the sperm surface, so that sperm are viable, motile, and capable of capacitating. Narrow cells are also positive for V-ATPase, thus thought to participate in lumen acidification (Pietrement *et al.*, 2006). In this scenario, it has been recently proposed that basal cells scan and sense the luminal environment of the epididymis, and participate in a cross talk with other epithelial cells, thus regulating their functions (Shum et al. 2008).

As shown in this work, the epididymides of cSrc null mice are small in size due to deficient development of their caudal regions. Although the diameter of the epididymal tubule appears to be normal, the size of clear cells is reduced in all regions, with the largest effect observed in the proximal cauda. In addition, the expression of two key transport proteins, the V-ATPase B1 subunit in clear cells, and AQP9 in principal cells is markedly reduced in cSrc null mice compared to expression in the epididymides of their normal siblings. cSrc is normally expressed in both principal and clear cells with higher amounts observed in clear cells. When localization studies were conducted in epididymides from mice of different age, it was observed that cSrc is initially expressed throughout the entire epididymis. However, in later developmental stages (4, 6 and 8 weeks), cSrc expression is enriched in clear cells. These results suggest that this tyrosine kinase plays a relevant role in clear cell differentiation. The reduced size of clear cells together with the reduced expression of V-ATPase in these cells are compatible with this notion. Altogether, these results indicate a critical role for cSrc in the establishment and/or maintenance of the differentiated phenotype of epithelial cells lining the distal regions of the epididymis (cauda) as well as the proximal ductus deferens.

The basic constituents of epididymal secretions are small vesicles known as epididymosomes, and non membranous components (Caballero et al. 2010). Epididymosomal formation involves epithelial cell apical region blebs that later detach along with a number of cytoskeleton proteins. The resulting vesicles constitute an extracellular form of protein trafficking, similar to exosome trafficking, delivering specific proteins to spermatozoa. Protein acquisition by epididymal sperm may account for their only means of protein content increase in these translationally inactive cells. Proteins in the epididymosomes that are transferred to sperm have a wide range of functions. For example, CRISP1, secreted by proximal epididymal segments, plays a role in sperm egg interaction in mouse, human and rat (Cohen et al. 2008;Busso et al. 2007). Glutathione peroxidase 5 (GPX5) is added to the spermatozoa in the proximal epididymal regions and protects spermatozoa from oxidative stress (Vernet et al. 2004). Interestingly, elimination of defective sperm might be aided through epididymosome ubiquitin transfer (Sutovsky et al. 2001). However, no reports until now have indicated the delivery of a specific protein involved in signaling events. In addition to defects in the cauda epididymis, we have

demonstrated here that cSrc is present in the membranous fraction of epididymal fluid, and that cSrc is present in spermatozoa only after they have undergone epididymal transit. Moreover, our data indicates that during spermatogenesis cSrc content is reduced to an almost undetectable level in condensed spermatids. These results are in agreement with cSrc mRNA expression levels, as it was previously shown that round spermatids contained only one third the level of cSrc mRNA detected in spermatogonia, and that this level is further decreased in elongated spermatids (Goupil et al. 2011). Although one report indicated the presence of cSrc in caput sperm (Baker et al. 2006), this discrepancy is likely due to contaminating vesicles in those preparations (see Fig. S3).

Consistent with previous results (Krapf et al. 2010;Baker et al. 2006), mature cauda epididymal sperm contain cSrc as revealed by western blot and immunofluorescence experiments. Importantly, in addition to standard controls (e.g. normal mouse serum), the specificity of the anti-cSrc antibody was evaluated using sperm and tissues from cSrc null mice. Interestingly, cSrc was detected in the flagellar midpiece and in the postacrosomal regions of the sperm head. Because the increase in tyrosine phosphorylation is mostly observed in the principal piece of the sperm flagellum, absence of cSrc in this compartment is consistent with previous conclusions that cSrc is not the tyrosine kinase responsible for the capacitation-associated changes in tyrosine phosphorylation (Krapf et al. 2010).

Although cSrc was found to be present in pachytene and round spermatids, no ultrastructural abnormalities were detected in cSrc null sperm, and the overall morphology of cSrc null seminiferous tubules, as well as the testes, is normal in appearance. On the other hand, cSrc null epididymides are smaller, indicating a role for cSrc in epididymal development. In particular, the cSrc null epididymal phenotype appears to be specific to the cauda epididymis, unlike other epididymal defects reported using genetically modified mice (Di Giovanni et al. 2011;Luo et al. 2011). As mentioned above, these observations suggest that sperm from these mice have functional defects associated with deficient epididymal maturation.

The observation that cSrc is acquired by spermatozoa during epididymal maturation is surprising, and raises a number of interesting questions: [1] what is the mechanism of cSrc acquisition by sperm; and [2] what is the role of cSrc in sperm function? A major possibility is that sperm cSrc derives from epididymal fluid, where it is present and is enriched in the fluid membranous vesicles known as epididymosomes. Epididymosomes are a type of exosome characterized by a high cholesterol/phospholipid ratio (Rejraji et al. 2006). In semen, similar vesicles primarily secreted by the prostate (known as “prostasomes”) have been described. A recent report has shown that prostasomes fuse to the sperm midpiece, transferring ryanodine receptors and secretory pathway Ca^{2+} ATPases that participate in progesterone-induced Ca^{2+} signaling (Park et al. 2011;Rejraji et al. 2006). Interestingly, cSrc kinase family members have been found in reticulocyte exosomes. It has been suggested that these proteins, and possibly lipid raft domains, might participate in molecule segregation during exosome formation in reticulocytes (de Gassart et al. 2003). Work from Robert Sullivan’s laboratory has indicated that epididymosomes fuse to the sperm plasma membrane through an active mechanism. This hypothesis is consistent with the restricted localization of cSrc in mature sperm.

In conclusion, the present study opens new avenues of study in the field of sperm developmental physiology: first, the phenotype of cSrc null mice has revealed that this tyrosine kinase is required for the development of the cauda epididymis and is most likely incorporated into sperm during epididymal maturation; and second, poor motility of sperm from cSrc null mice together with the inability of these sperm to fertilize eggs both in vitro

and in vivo have indicated that this enzyme could be essential for sperm function in the fertilization process.

Supplementary Material

Refer to Web version on PubMed Central for supplementary material.

Acknowledgments

This work was supported by NIH: R01 HD44044 and HD038082 (to PEV), HD40793, HD45821 and DK38452 (to SB), National Agency for Scientific and Technological Promotion of Argentina PICT 633 and WHO H9-TSA-037 (to PSC) and by a Lalor Foundation postdoctoral fellowship (to YCR). We would also like to thank Dr. Paula Stein for her assistance in in vitro fertilization experiments. Authors declare no conflict of interests.

REFERENCES

Abascal I, Skalaban SR, Grimm KM, Aviles M, Martianez-Menarguez JA, Castells MT, Ballesta J, Alhadeff JA. Alteration of the isoform composition of plasma-membrane-associated rat sperm alpha-L-fucosidase during late epididymal maturation: comparative characterization of the acidic and neutral isoforms. Biochem.J. 1998; 333(Pt 1):201–207. [PubMed: 9639580]

Amling M, Neff L, Priemel M, Schilling AF, Rueger JM, Baron R. Progressive increase in bone mass and development of odontomas in aging osteopetrotic c-src-deficient mice. Bone. 2000; 27:603–610. [PubMed: 11062345]

Badran HH, Hermo LS. Expression and regulation of aquaporins 1, 8, and 9 in the testis, efferent ducts, and epididymis of adult rats and during postnatal development. J.Androl. 2002; 23:358–373. [PubMed: 12002438]

Baker MA, Hetherington L, Aitken RJ. Identification of SRC as a key PKA-stimulated tyrosine kinase involved in the capacitation-associated hyperactivation of murine spermatozoa. J.Cell Sci. 2006; 119:3182–3192. [PubMed: 16835269]

Bellve AR, Millette CF, Bhatnagar YM, O'Brien DA. Dissociation of the mouse testis and characterization of isolated spermatogenic cells. J.Histochem.Cytochem. 1977; 25:480–494. [PubMed: 893996]

Brown D, Lydon J, McLaughlin M, Stuart-Tilley A, Tyszkowski R, Alper S. Antigen retrieval in cryostat tissue sections and cultured cells by treatment with sodium dodecyl sulfate (SDS). Histochem.Cell Biol. 1996; 105:261–267. [PubMed: 9072183]

Busso D, Cohen DJ, Maldera JA, Dematteis A, Cuasnicu PS. A novel function for CRISP1 in rodent fertilization: involvement in sperm-zona pellucida interaction. Biol.Reprod. 2007; 77:848–854. [PubMed: 17671267]

Caballero J, Frenette G, Sullivan R. Post testicular sperm maturational changes in the bull: important role of the epididymosomes and prostasomes. Vet.Med.Int. 2010; 2011 757194.

Cohen DJ, Busso D, Da RV, Ellerman DA, Maldera JA, Goldweic N, Cuasnicu PS. Participation of cysteine-rich secretory proteins (CRISP) in mammalian sperm-egg interaction. Int.J.Dev.Biol. 2008; 52:737–742. [PubMed: 18649285]

Cornwall GA. New insights into epididymal biology and function. Hum.Reprod.Update. 2009; 15:213–227. [PubMed: 19136456]

Da Silva N, Pisitkun T, Belleannee C, Miller LR, Nelson R, Knepper MA, Brown D, Breton S. Proteomic analysis of V-ATPase-rich cells harvested from the kidney and epididymis by fluorescence-activated cell sorting. Am.J.Physiol Cell Physiol. 2010; 298:C1326–C1342. [PubMed: 20181927]

de Gassart A, Geminard C, Fevrier B, Raposo G, Vidal M. Lipid raft-associated protein sorting in exosomes. Blood. 2003; 102:4336–4344. [PubMed: 12881314]

Di Giovanni V, Alday A, Chi L, Mishina Y, Rosenblum ND. Alk3 controls nephron number and androgen production via lineage-specific effects in intermediate mesoderm. Development. 2011; 138:2717–2727. [PubMed: 21613322]

Donepudi M, Resh MD. c-Src trafficking and co-localization with the EGF receptor promotes EGF ligand-independent EGF receptor activation and signaling. Cell Signal. 2008; 20:1359–1367. [PubMed: 18448311]

Elkjaer M, Vajda Z, Nejsum LN, Kwon T, Jensen UB, Amiry-Moghaddam M, Frokiaer J, Nielsen S. Immunolocalization of AQP9 in liver, epididymis, testis, spleen, and brain. Biochem.Biophys.Res.Commun. 2000; 276:1118–1128. [PubMed: 11027599]

Frenette G, Sullivan R. Prostasome-like particles are involved in the transfer of P25b from the bovine epididymal fluid to the sperm surface. Mol.Reprod.Dev. 2001; 59:115–121. [PubMed: 11335953]

Goupil S, La Salle S, Trasler JM, Bordeleau LJ, Leclerc P. Developmental expression of SRC-related tyrosine kinases in the mouse testis. J.Androl. 2011; 32:95–110. [PubMed: 20798388]

Kalab P, Visconti P, Leclerc P, Kopf GS. p95, the major phosphotyrosine-containing protein in mouse spermatozoa, is a hexokinase with unique properties. J.Biol.Chem. 1994; 269:3810–3817. [PubMed: 7508920]

Kirichok Y, Navarro B, Clapham DE. Whole-cell patch-clamp measurements of spermatozoa reveal an alkaline-activated Ca2+ channel. Nature. 2006; 439:737–740. [PubMed: 16467839]

Krapf D, Arcelay E, Wertheimer EV, Sanjay A, Pilder SH, Salicioni AM, Visconti PE. Inhibition of Ser/Thr phosphatases induces capacitation-associated signaling in the presence of Src kinase inhibitors. J.Biol.Chem. 2010; 285:7977–7985. [PubMed: 20068039]

Laemmli UK. Cleavage of structural proteins during the assembly of the head of bacteriophage T4. Nature. 1970; 227:680–685. [PubMed: 5432063]

Luo J, Gupta V, Kern B, Tash JS, Sanchez G, Blanco G, Kinsey WH. Role of FYN Kinase in Spermatogenesis: Defects Characteristic of Fyn-Null Sperm in Mice. Biol.Reprod. 2011

Moore GD, Ayabe T, Visconti PE, Schultz RM, Kopf GS. Roles of heterotrimeric and monomeric G proteins in sperm-induced activation of mouse eggs. Development. 1994; 120:3313–3323. [PubMed: 7720569]

Nakanishi T, Ikawa M, Yamada S, Parvinen M, Baba T, Nishimune Y, Okabe M. Real-time observation of acrosomal dispersal from mouse sperm using GFP as a marker protein. FEBS Lett. 1999; 449:277–283. [PubMed: 10338148]

Park KH, Kim BJ, Kang J, Nam TS, Lim JM, Kim HT, Park JK, Kim YG, Chae SW, Kim UH. Ca2+ signaling tools acquired from prostasomes are required for progesterone-induced sperm motility. Sci.Signal. 2011; 4:ra31. [PubMed: 21586728]

Pastor-Soler N, Bagnis C, Sabolic I, Tyszkowski R, McKee M, Van Hoek A, Breton S, Brown D. Aquaporin 9 expression along the male reproductive tract. Biol.Reprod. 2001; 65:384–393. [PubMed: 11466204]

Pastor-Soler N, Isnard-Bagnis C, Herak-Kramberger C, Sabolic I, Van Hoek A, Brown D, Breton S. Expression of aquaporin 9 in the adult rat epididymal epithelium is modulated by androgens. Biol.Reprod. 2002; 66:1716–1722. [PubMed: 12021052]

Pastor-Soler NM, Fisher JS, Sharpe R, Hill E, Van Hoek A, Brown D, Breton S. Aquaporin 9 expression in the developing rat epididymis is modulated by steroid hormones. Reproduction. 2010; 139:613–621. [PubMed: 19948840]

Pietrement C, Da Silva N, Silberstein C, James M, Marsolais M, Van Hoek A, Brown D, Pastor-Soler N, Ameen N, Laprade R, Ramesh V, Breton S. Role of NHERF1, cystic fibrosis transmembrane conductance regulator, and cAMP in the regulation of aquaporin 9. J.Biol.Chem. 2008; 283:2986–2996. [PubMed: 18055461]

Pilder SH, Olds-Clarke P, Phillips DM, Silver LM. Hybrid sterility-6: a mouse t complex locus controlling sperm flagellar assembly and movement. Dev.Biol. 1993; 159:631–642. [PubMed: 8405685]

Platt MD, Salicioni AM, Hunt DF, Visconti PE. Use of differential isotopic labeling and mass spectrometry to analyze capacitation-associated changes in the phosphorylation status of mouse sperm proteins. J.Proteome.Res. 2009; 8:1431–1440. [PubMed: 19186949]

Rejraji H, Sion B, Prensier G, Carreras M, Motta C, Frenoux JM, Vericel E, Grizard G, Vernet P, Drevet JR. Lipid remodeling of murine epididymosomes and spermatozoa during epididymal maturation. Biol.Reprod. 2006; 74:1104–1113. [PubMed: 16510839]

Robaire, B.; Hinton, BT.; Orgebin-Crist, MC. The epididymis. Neill, JD., editor. New York, NY: Physiology of Reproduction Elsevier; 2006. p. 1071-1148.

Schwartzberg PL, Xing L, Hoffmann O, Lowell CA, Garrett L, Boyce BF, Varmus HE. Rescue of osteoclast function by transgenic expression of kinase-deficient Src in src-/- mutant mice. Genes Dev. 1997; 11:2835–2844. [PubMed: 9353253]

Shum WW, Da Silva N, McKee M, Smith PJ, Brown D, Breton S. Transepithelial projections from basal cells are luminal sensors in pseudostratified epithelia. Cell. 2008; 135:1108–1117. [PubMed: 19070580]

Shum WW, Ruan YC, Da Silva N, Breton S. Establishment of cell-cell cross talk in the epididymis: control of luminal acidification. J.Androl. 2011; 32:576–586. [PubMed: 21441423]

Soriano P, Montgomery C, Geske R, Bradley A. Targeted disruption of the c-src proto-oncogene leads to osteopetrosis in mice. Cell. 1991; 64:693–702. [PubMed: 1997203]

Sullivan R, Frenette G, Girouard J. Epididymosomes are involved in the acquisition of new sperm proteins during epididymal transit. Asian J.Androl. 2007; 9:483–491. [PubMed: 17589785]

Sutovsky P, Moreno R, Ramalho-Santos J, Dominko T, Thompson WE, Schatten G. A putative, ubiquitin-dependent mechanism for the recognition and elimination of defective spermatozoa in the mammalian epididymis. J.Cell Sci. 2001; 114:1665–1675. [PubMed: 11309198]

Vernet P, Aitken RJ, Drevet JR. Antioxidant strategies in the epididymis. Mol.Cell Endocrinol. 2004; 216:31–39. [PubMed: 15109742]

Visconti PE, Krapf D, De La Vega-Beltran JL, Acevedo JJ, Darszon A. Ion channels, phosphorylation and mammalian sperm capacitation. Asian J.Androl. 2011; 13:395–405. [PubMed: 21540868]

Visconti PE, Moore GD, Bailey JL, Leclerc P, Connors SA, Pan D, Olds-Clarke P, Kopf GS. Capacitation of mouse spermatozoa. II. Protein tyrosine phosphorylation and capacitation are regulated by a cAMP-dependent pathway. Development. 1995; 121:1139–1150. [PubMed: 7538069]

Wertheimer EV, Salicioni AM, Liu W, Trevino CL, Chavez J, Hernandez-Gonzalez EO, Darszon A, Visconti PE. Chloride Is essential for capacitation and for the capacitation-associated increase in tyrosine phosphorylation. J.Biol.Chem. 2008; 283:35539–35550. [PubMed: 18957426]

HIGHLIGHTS

1. Sperm from cSrc null mice show poor motility and are unable to fertilize *in vitro*.
2. Src KO males have a developmental defect in the last section of their epididymides
3. Testicular sperm are devoid of cSrc.
4. cSrc is incorporated into sperm during epididymal transit

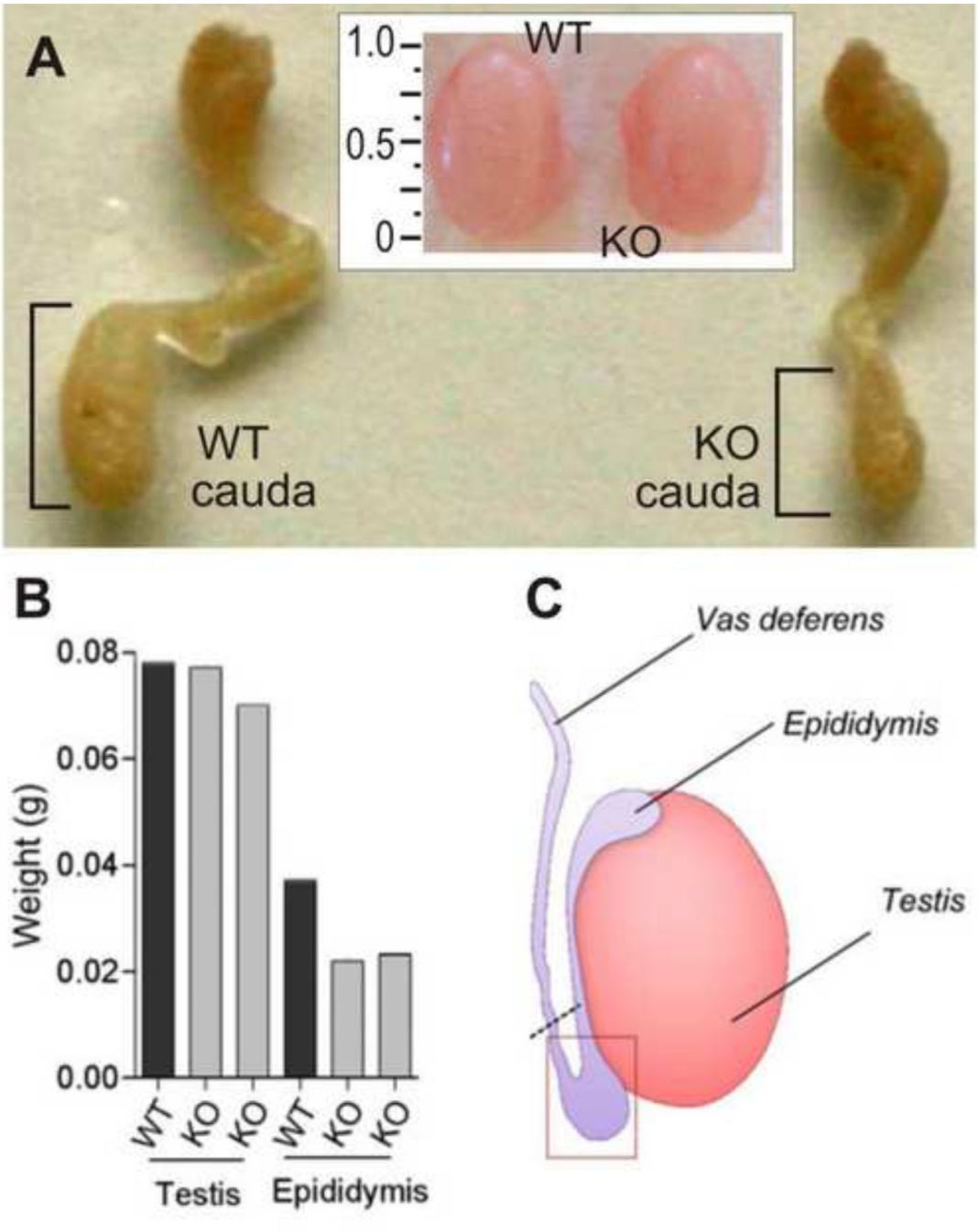

Figure 1. Weight of testis and epididymis of cSrc null (KO) mice compared to wild type (WT)

A and B, testis weight is not affected by deletion of cSrc, but the epididymis is significantly smaller and lighter in cSrc KO mice compared to WT. ***C***: Diagram representing the testis and epididymis; the cauda (***C***, boxed) is the most affected region of the epididymis.

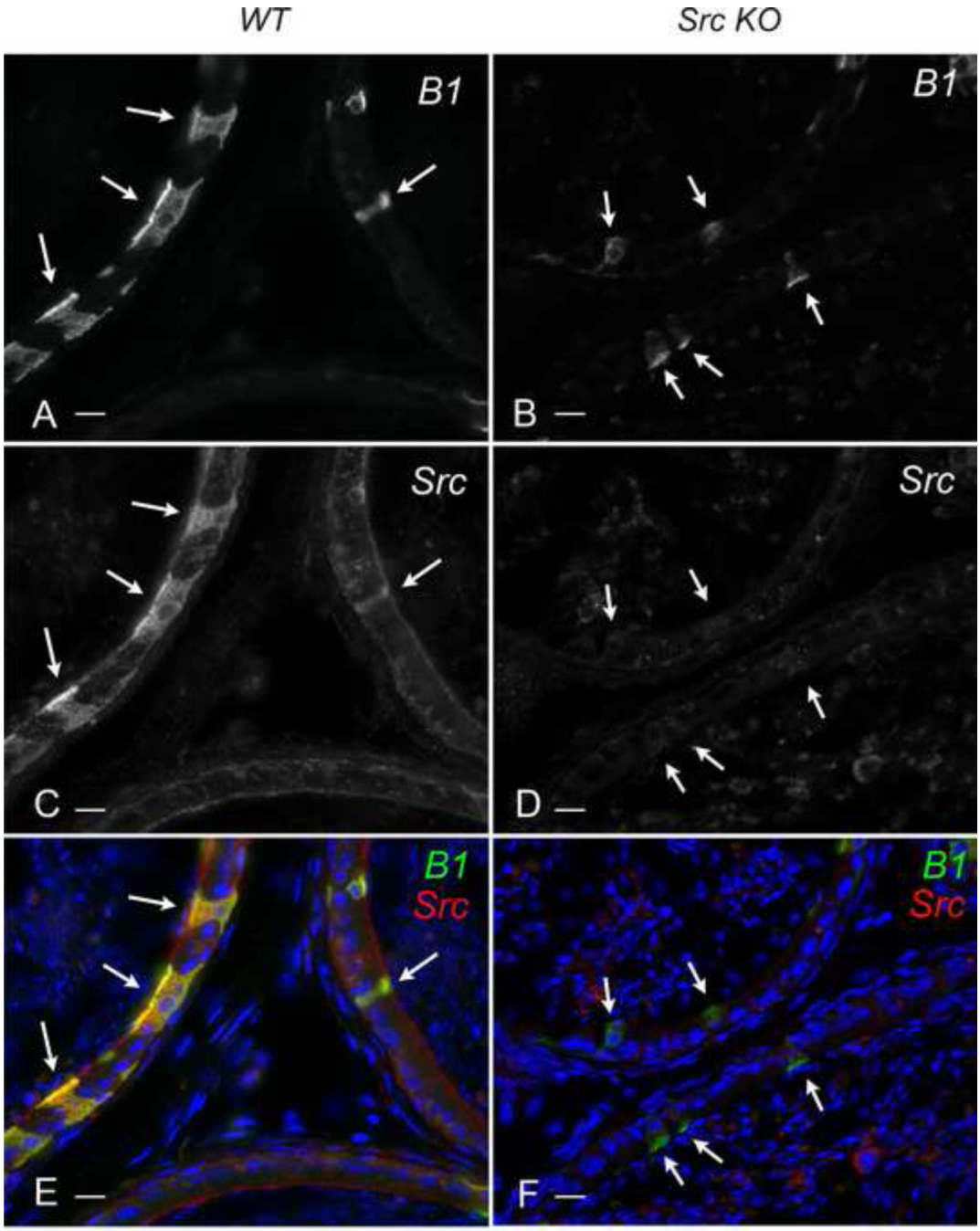

Figure 2. Expression pattern of cSrc in cauda epididymal tubules

A–F, epididymides from WT and cSrc KO mice were double-labeled for the V-ATPase B1 subunit (B1: ***A, B***) and cSrc (Src; ***C, D***). In WT epididymis (***C***), strong cSrc labeling was detected in clear cells (arrows), identified by their positive labeling for B1 (***A***). ***E***, the yellow fluorescence in this merged panel indicates co-expression of B1 and cSrc in clear cells. A weaker cSrc labeling was also detected in principal cells in WT mice (***C, E***). ***B, D, F***, in cSrc KO epididymides, as expected no cSrc staining was observed in epithelial cells. Only occasional cells displayed faint autofluorescence in the interstitium. Clear cells appear

smaller and show a weaker staining for the V-ATPase B1 subunit (***B***) compared to WT (***A***). Bars = 10 μm.

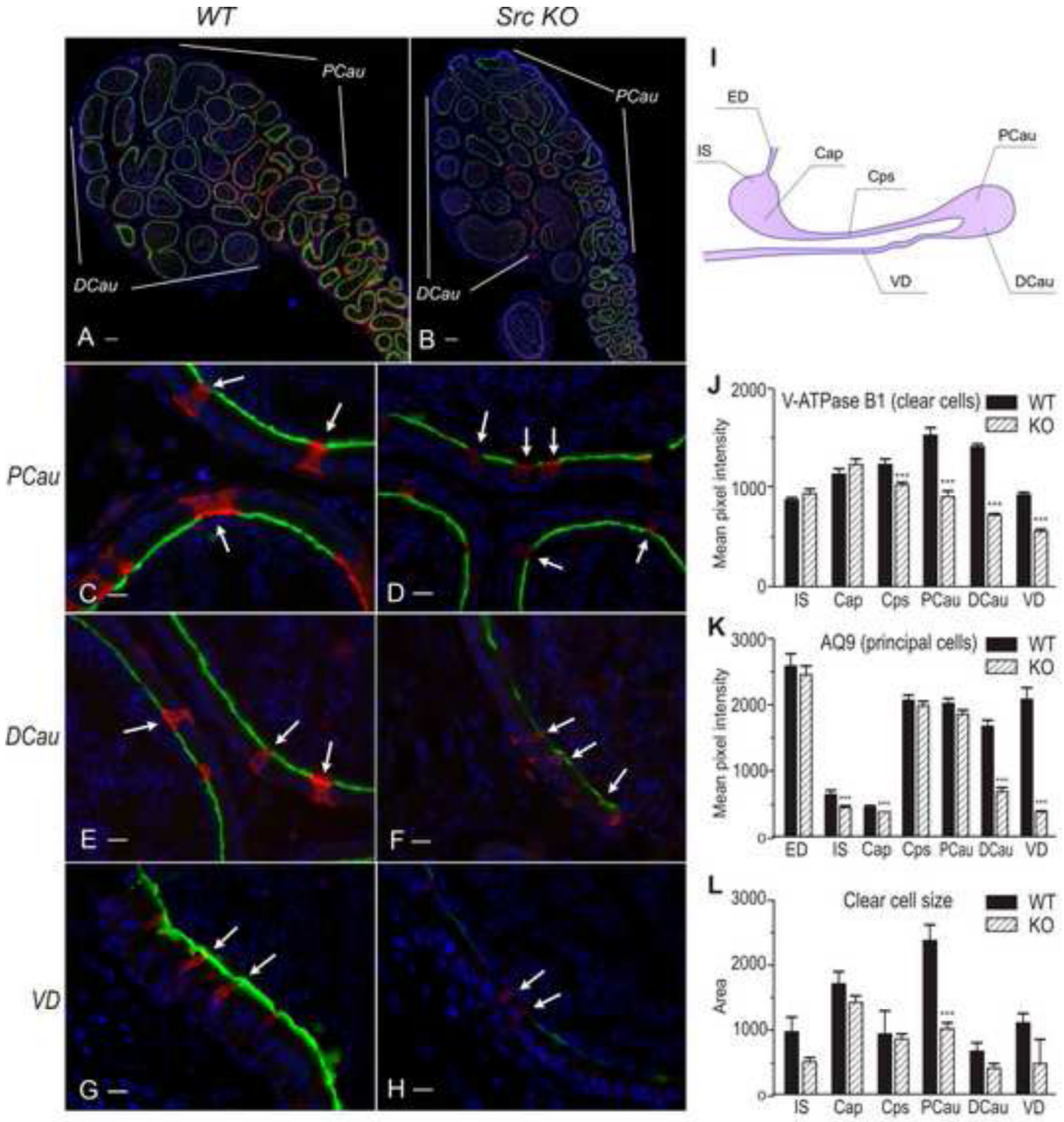

Figure 3. Expression of principal cell (AQP9, green stained) and clear cell (V-ATPase B1 subunit, red stained) markers in the epididymis of cSrc KO mice compared to WT mice

A and B, low magnification pictures of cauda epididymidides from WT (***A***) and cSrc KO (***B***) mice ***C and D***, micrographs of the proximal cauda epididymides (*PCau*) showed a weaker label for the V-ATPase B1 subunit was observed in cSrc KO versus WT (arrows). ***E and F***, in the distal cauda (*DCau*), reduced fluorescence was detected for both AQP9 in principal cells and V-ATPase B1 in clear cells (arrows) in cSrc KO compared to WT mice. ***G and H***, weaker labeling was also detected for AQP9 in principal cells and V-ATPase B1 in clear cells (arrows) in the proximal ductus (vas) deferens (VD) in cSrc KO compared to WT mice. Nuclei were labeled with DAPI. ***I***, diagram indicating different regions of the

epididymis: initial segment (IS), caput (Cap), corpus (Cps), proximal cauda (PCau), distal cauda (DC) and vas deferens (VD). ***J***, Significant decreases in V-ATPase B1 labeling intensity were detected in clear cells of the corpus (Cps), proximal cauda (PCau), distal cauda (DCau) and proximal vas deferens (VD) in Src KO versus WT mice. ***K***, significant decreases in AQP9 labeling intensity were detected in the distal cauda (DCau) and proximal vas deferens (VD) in cSrc KO versus WT mice. ***L***, smaller clear cells in cSrc KO compared to WT mice was observed in all epididymal regions. Mean ± SEM; *** $p < 0.001$. Bars=100 μm (***A, B***); 10 μm (***C–H***).

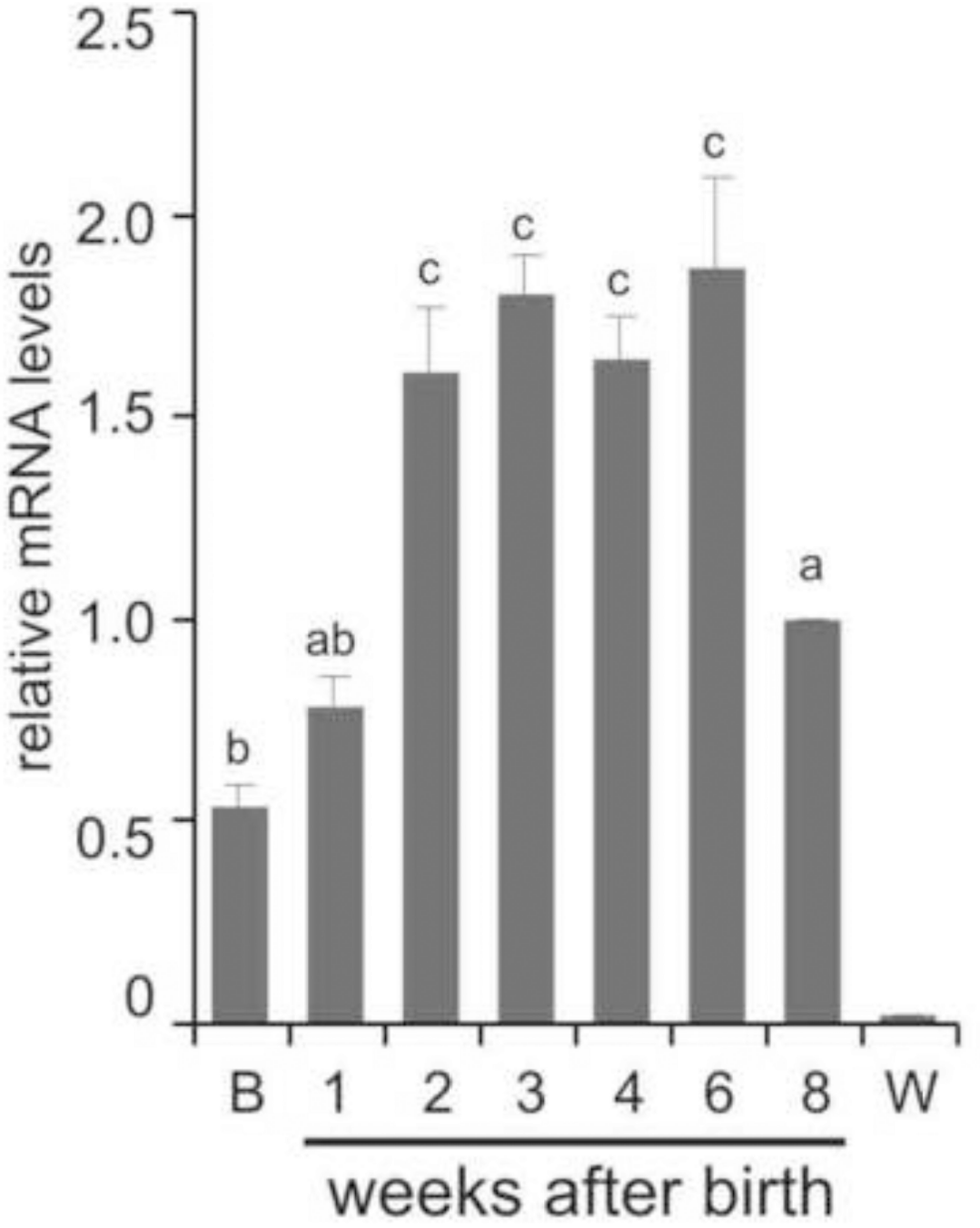

Figure 4. Expression of cSrc during post natal stages

Quantitative RT-PCR analysis of cSrc mRNA during 1–8 weeks after birth. Brain (B) was used as positive control and water (W) as negative control. Expression levels were normalized to week 8. Data represent mean ± SEM, of two replicates performed in triplicates. Means of groups that have different letters differ significantly ($p<0.001$)..

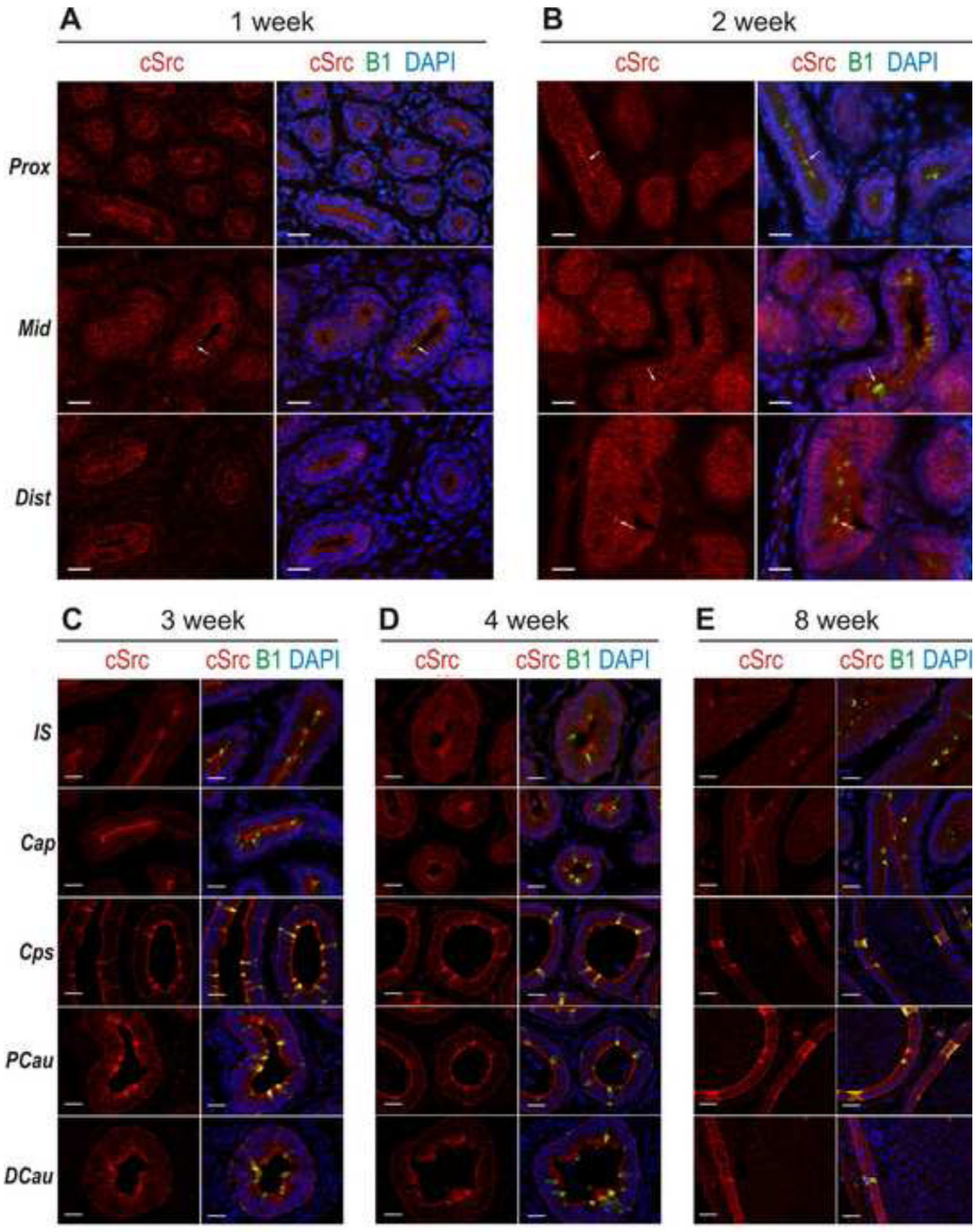

Figure 5. Histochemical analysis of cSrc expression in mouse epididymis at postnatal weeks 1 through 8

Double-labeling for cSrc (*red*) and V-ATPase B1 subunit (B1, *green*). ***A and B***, proximal, middle and distal epididymal regions of 1-week (***A***) and 2-week (***B***) mice. cSrc is detected in all epithelial cells throughout the entire epididymis. A B1-labeled clear cell is visible in the middle region at postnatal week 1 (***A***, arrow). At postnatal week 2, B1-labeled clear cells are observed in all epididymal regions (***B***, arrows). ***C–E***, initial segments (IS), caput (Cap), corpus (Cps), proximal cauda (Pcau) and distal cauda (Dcau) from mice at postnatal weeks 3 (***C***), 4 (***D***) and 8 (***E***). At weeks 3 and 4, cSrc was detected in clear cells (B1 positive) and principal cells in all segments, where it is enriched in the apical membrane. At week 8, when

mice reach puberty, the cSrc apical membrane labeling of principal cells decreased in some regions IS, CPS and DCau. Nuclei were labeled with DAPI (*Blue*). Bars = 20 μm.

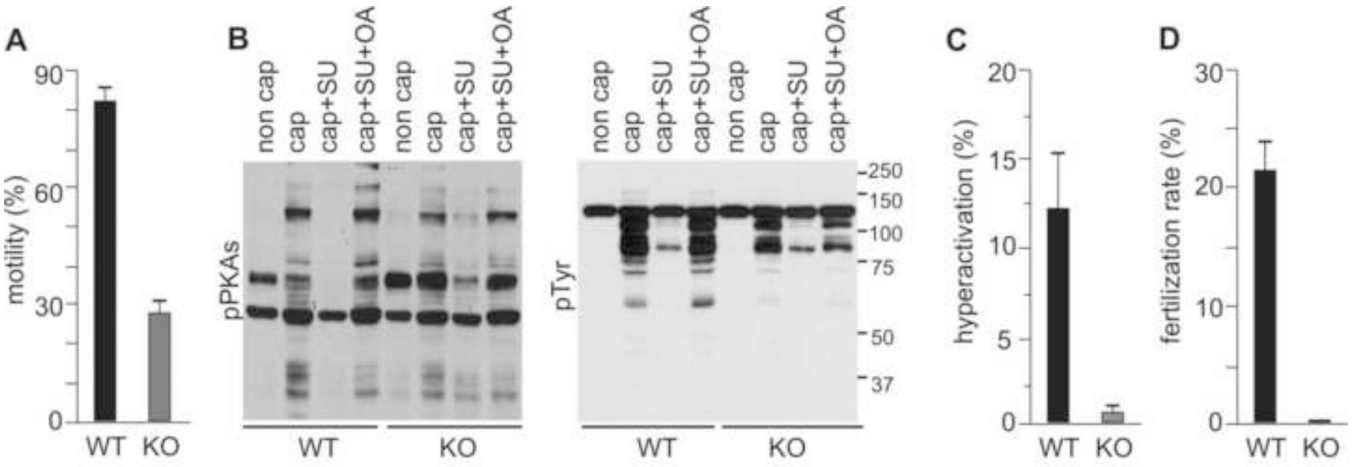

Figure 6. Capacitation parameters of cSrc null mice

A, total motility of non capacitated mouse sperm from cSrc-null (KO) and wild-type (WT) siblings was examined using the CASA system. No ultrastructural alterations that might explain the motility defects were observed in KO spermatozoa when compared to wild-type spermatozoa (see Fig. S1). Data represent mean ± S.E.M, n=3. ***B***, sperm from cSrc-null (KO) and wild-type (WT) siblings were incubated under non-capacitating and capacitating conditions in the presence of either 50 μM SU6656 alone or with addition of 1 nM okadaic acid (OA) for 60 min. Protein extracts were analyzed by Western blot with anti-pY (clone 4G10) and anti-phosphoPKA-substrate antibodies. ***C***, hyperactivated motility of capacitated mouse sperm from cSrc-null (KO) and wild-type (WT) siblings was examined using the CASA system. Data represent mean ± S.E.M, n=3. ***D***, sperm from cSrc-null (KO) and wild-type (WT) siblings were capacitated and used to inseminate WT mouse eggs. Data represent mean ± s.e.m., n=3. At least 30 eggs were evaluated in each treatment.

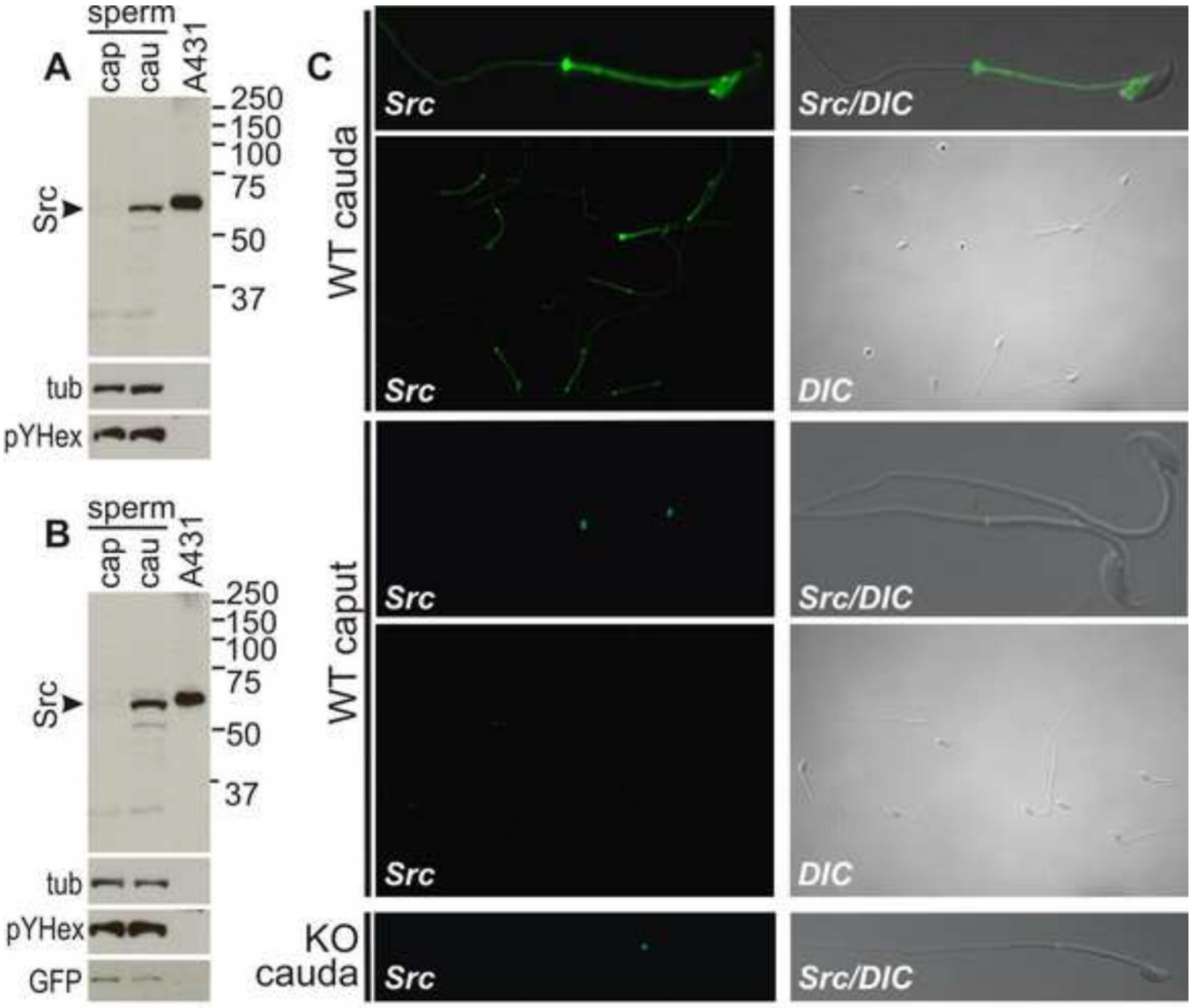

Figure 7. Presence and localization of c-Src in epididymal sperm

A and B, immunodetection of c-Src in cauda and caput sperm extracts from WT mice (***A***) and Acr-GFP mice (***B***), expressing GFP in their acrosomes. A431 cells were used as positive controls (1 μg of total protein). Equal loading controls were performed with anti-tubulin, anti-pTyr in order to detect Hexokinase, and with anti-GFP (panel ***B***). The status of the acrosome was unaffected by percoll purification in either caput or cauda sperm (see Fig. S2). ***C***, c-Src was immunolocalized in cauda sperm. Only non-specific signal was observed in both caput sperm and cSrc-null mice cauda sperm. Right panels show either DIC or fluorescence/DIC merged images.

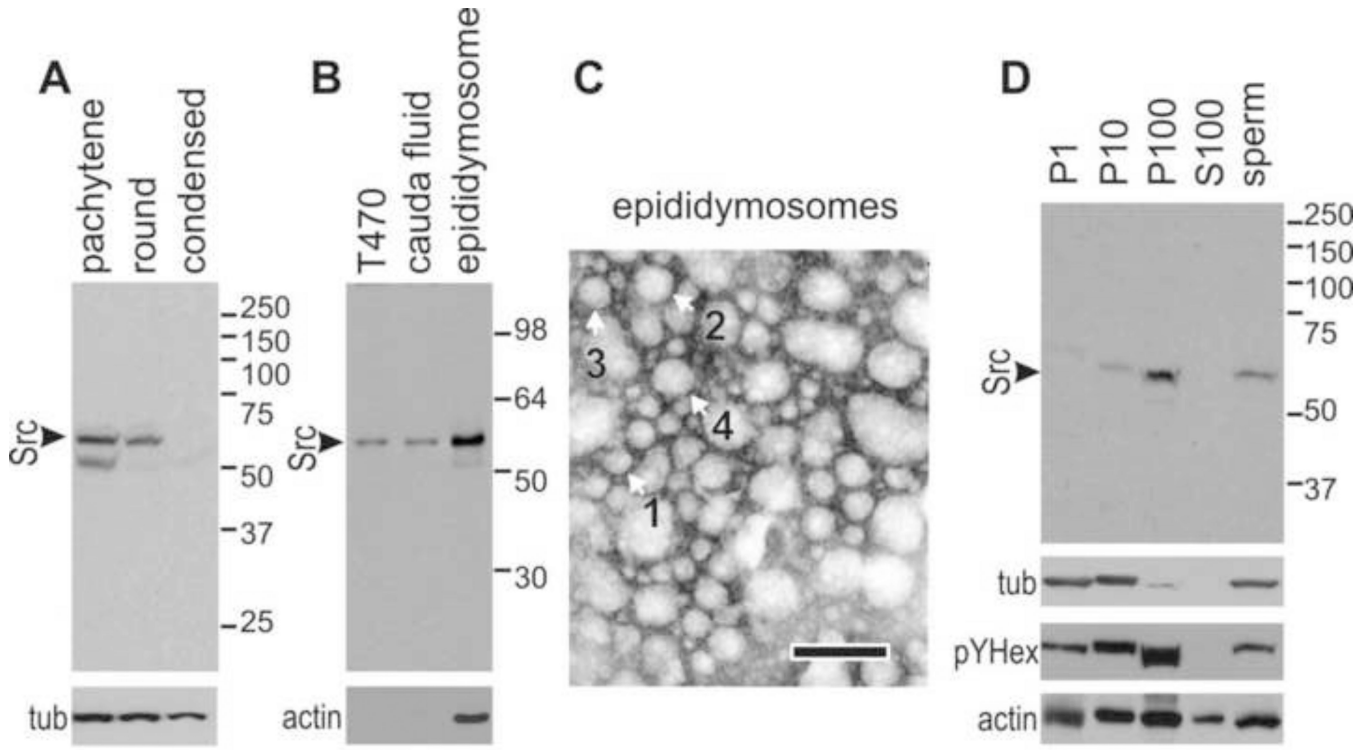

Figure 8. Presence of cSrc in spermatids, epididymal fluid and mature sperm

A, c-Src presence was analyzed in spermatogenic cells. cSrc kinase is present in pachytene cells, but it decreases in round spermatids and is nearly undetectable in condensed spermatids. ***B***, cSrc is enriched in epididymosome fraction from cauda fluid. Positive control was performed with T470 cells (10 μg of total protein), and 20 μg of cauda fluid proteins and 10 μg of total epididymosome proteins were loaded. ***C***, Transmission electron micrograph showing epididymosome enriched fraction of cauda fluid. Numbers indicate four different vesicles with the following diameters in nm: *1*, 58.4; *2*, 75.7; *3*, 69.6; *4*, 89.1. Bar represents 200 nm. ***D***, Non-capacitated sperm were homogenized as described in Methods, and 1,000 × *g* pellet (P1), 10,000 × *g* pellet (P10), 100,000 × *g* pellet (P100) and 100,000 × *g* supernatant (S100) fractions were prepared. 30 μg of proteins of each fraction were separated by SDS-PAGE and subjected to immunoblotting using anti-Src. cSrc is localized to the membrane fraction of cauda epididymal sperm. Controls were performed with anti-tubulin, anti-phosphoTyr, and anti-actin antibodies.

Table 1
Motility parameters by Computer Aided Sperm Analysis

Sperm motility parameters are affected in Src KO mice
Caudal sperm from either KO or WT siblings were incubated for 60 min in medium that supports capacitation, in the presence of okadaic acid (OA, 100 nM) when indicated. After capacitation, sperm motility was examined using the CEROS computer-assisted semen analysis (CASA) system. Data represent mean ± s.e.m., n=3. VAP, velocity average path; VSL, velocity straight line, VCL, velocity curvilinear

	VAP(μm/s)	VSL(μm/s)	VCL(μm/s)	prog(%)
cauda WT	72 ± 4.9	45 ± 3.9	152 ± 5.2	14 ± 2.2
cauda KO	28 ± 2.4*	15 ± 2.8*	51 ± 4.3*	6.7 ± 1.8*
cauda KO+OA	30 ± 1.1*	18 ± 1.5*	53 ± 3.9*	7.1 ± 1.1*